A nonstationary ENSO-NAO relationship due to AMO modulation

A Nonstationary ENSO-NAO relationship due to AMO modulation

Wenjun Zhang[1], Xuebin Mei[1], Xin Geng[1], Andrew G. Turner[2,3], Fei-Fei Jin[4]

[1]CIC-FEMD/ILCEC, Key Laboratory of Meteorological Disaster of Ministry of Education, Nanjing University of Information Science and Technology, Nanjing 210044, China

[2]National Center for Atmospheric Science, University of Reading, Reading RG6 6BB, UK

[3]Department of Meteorology, University of Reading, Reading RG6 6BB, UK

[4]Department of Atmospheric Sciences, SOEST, University of Hawai'i at Manoa, Honolulu, HI 96822, USA

Jun 2, 2018

(*Submitting to Journal of Climate*)

Corresponding author address:

Dr. Wenjun Zhang

College of Atmospheric Sciences, Nanjing University of Information Science and Technology, Nanjing 210044, China.

E-mail: zhangwj@nuist.edu.cn

Abstract

Many previous studies have demonstrated a high uncertainty in the relationship between the El Niño-Southern Oscillation (ENSO) and North Atlantic Oscillation (NAO). In the present work, decadal modulation by the Atlantic Multidecadal Oscillation (AMO) is investigated as a possible cause of the nonstationary ENSO-NAO relationship based on observed and reanalysis data. It is found that the negative ENSO-NAO correlation in late winter is significant only when ENSO and the AMO are in-phase (AMO+/El Niño and AMO-/La Niña). However, no significant ENSO-driven atmospheric anomalies can be observed over the North Atlantic when ENSO and the AMO are out-of-phase (AMO-/El Niño and AMO+/La Niña). Further analysis indicates that the sea surface temperature anomaly (SSTA) in the tropical North Atlantic (TNA) plays an essential role in this modulating effect. Due to broadly analogous TNA SSTA responses to both ENSO and the AMO during late winter, a warm SSTA in the TNA is evident when El Niño occurs during a positive AMO phase, resulting in a significantly weakened NAO, and vice versa when La Niña occurs during a negative AMO phase. In contrast, neither the TNA SSTA nor the NAO show a prominent change under out-of-phase combinations of ENSO and AMO. The AMO modulation and associated effect of the TNA SSTA are shown to be well reproduced by historical simulations of the HadCM3 coupled model and further verified by forced experiments using an atmospheric circulation model. These offer hope that similar models will be able to make predictions for the NAO when appropriately initialized.

1. Introduction

As the dominant low-frequency atmospheric circulation variability in the extratropical Northern Hemisphere, the North Atlantic Oscillation (NAO) has extensive and pronounced climate impacts around the globe (e.g., Hurrell 1995, 2003; Cattiaux et al. 2010; Cohen et al. 2012; Li et al. 2013, 2018). The NAO explains much of the observed temperature variability over Eurasia and North America (e.g., Hurrell 1996; Wang et al. 2010), and its decadal variation also plays a role in the recent decline of Arctic sea ice concentration (Deser and Teng 2008). To date, more and more attention has been paid to understanding NAO variability and its drivers in order to improve seasonal-to-interannual prediction of the NAO itself and associated impacts (e.g., Johansson 2007; Dunstone et al. 2016; Smith et al. 2016). On interannual timescales, possible influences of the El Niño-Southern Oscillation (ENSO) on the NAO have been extensively studied, since ENSO is one of the largest modes of interannual variability in the coupled Earth system.

ENSO exerts its influence on the global climate mostly through so-called atmospheric bridge mechanisms (e.g., Klein et al. 1999; Alexander et al. 2002; Lau and Nath 2003; Graf and Zanchettin 2012; Zhang et al. 2015). While the climate responses to ENSO in the North Pacific and North America regions are well understood (e.g., Hoskins and Karoly 1981; Wallace and Gutzler 1981; Infanti and Kirtman 2016), the physical linkages between ENSO and climate variability over the North Atlantic-European sector are still unclear. Early studies argued that signals of ENSO are almost absent in North Atlantic/European climate variability (e.g., Ropelewski and Halpert 1987; Halpert and Ropelewski 1992). This viewpoint is challenged by subsequent studies, which demonstrated an ENSO signal in Europe albeit with large inter-event diversity (e.g., Fraedrich 1994; Gouirand and Moron 2003; Brönnimann et al. 2007a,b), possibly due to the existence of two types of ENSO (Graf and Zanchettin 2012; Zhang et al. 2015, 2018) and prominent sub-seasonal variations (e.g., Fraedrich and Muller 1992; Moron and Gouirand 2003; Geng et al. 2017). Various observational and modeling studies have demonstrated that El Niño events usually coincide with a negative NAO-like atmospheric anomaly pattern during the late winter season, with a colder and drier than normal climate over Northern Europe (e.g., Mathieu et al. 2004; Brönnimann et al. 2007a,b). The responses to La Niña events are approximately opposite in sign to those of El Niño. Nevertheless, the dynamical mechanisms addressing how ENSO-related tropical sea surface temperature (SST) anomalies (SSTA) influence the NAO variability are still under debate. It has been proposed that the atmosphere over the North Pacific may serve as a bridge linking ENSO-associated diabatic heating in the tropical Pacific with atmospheric circulation anomalies over the North Atlantic (e.g., Wu and Hsieh 2004; Graf and Zanchettin 2012; Zhang et al. 2015, 2018). ENSO-forced synoptic eddies over the eastern Pacific and North America could modulate the meridional propagation of synoptic wave packets over the North Atlantic, and then favor the occurrence of different NAO phases (e.g., Li and Lau 2012a, b; Drouard et al. 2015). The stratosphere might also act as a mediator to connect the signal between the Pacific and Atlantic basins (e.g., Castanheira and Graf 2003; Ineson and Scaife 2009;

Bell et al. 2009). As an additional pathway, some previous studies reported that the delayed tropical Atlantic SSTA following the ENSO peak could also affect the North Atlantic atmospheric circulation (e.g., Watanabe and Kimoto 1999; Robertson et al. 2000; Peng et al. 2005; Li et al. 2007; Davini et al. 2015).

Many studies show that the NAO also displays prominent decadal variability, which may be associated with the underlying low-frequency SST forcing. In particular, the linkage between the NAO and the Atlantic multidecadal oscillation (AMO; Peings and Magnusdottir 2014; Omrani et al. 2014) has been widely explored, since the AMO has been recognized as an important driver of Northern Hemisphere climate variability (e.g., Kerr 2000; Enfield et al. 2001; Zhang et al. 2007; Sun et al. 2011; Sun et al. 2015). A warm AMO phase usually accompanies occurrence of more frequent negative NAO and thus more cold days over Europe and North America (e.g., Ting et al. 2011, 2014; Kavvada et al. 2013; Peings and Magnusdottir 2014). Therefore, it is compelling to hypothesize that the AMO may in some way act to modulate the ENSO-NAO relationship.

Since any modulation of the ENSO-NAO relationship by the AMO has not been sufficiently elucidated in the aforementioned studies, in this study we investigate the influence of phase combinations of the ENSO and AMO on the NAO based on long-term observational datasets and model simulations. Our results will show that the AMO causes significant modulation of the ENSO-NAO relationship. Furthermore, the physical mechanisms behind this AMO modulation effect are also proposed. In the remainder of the paper, Section 2 introduces the observational datasets, model simulations and methodologies. The modulation effect of the ENSO-NAO relationship by the AMO is illustrated in Section 3. In Section 4, we propose the possible mechanisms for modulation, and further use historical HadCM3 model simulations as well as atmospheric general circulation model (AGCM) experiments based on Geophysical Fluid Dynamics Laboratory (GFDL) global Atmospheric Model version 2.1 (AM2.1) to validate our hypotheses. Finally, a summary and discussion of the results are presented in Section 5.

2. Datasets and Methods and experimental design

2.1 Datasets and Methods

The monthly datasets used in this study include global SST derived from the National Oceanic and Atmospheric Administration (NOAA) Extended Reconstructed SST analysis, version 3 (ERSST v3b) from 1950 to 2016 (Smith et al. 2008). Atmospheric circulations are examined based on the National Environmental Prediction Center/National Center for the Atmospheric Research (NCEP/NCAR) monthly reanalysis data from 1950 to 2016 (Kalnay et al. 1996) and Twentieth Century Reanalysis (20CR) monthly data from 1900 to 2012 (Compo et al. 2010). To describe the NAO-associated atmospheric activity, the NAO index is defined as the difference in normalized zonal-averaged sea-level pressure (SLP) over the North Atlantic region (80°W-30°E) between 35°N and 65°N (Li et al. 2003). The AMO index is calculated as the area-averaged SSTA over the North Atlantic region (0°-60°N, 0°-80°W) (Trenberth and Shea 2006).

ENSO events usually reach their peak during boreal winter (December-January-February, DJF), and the relatively stable NAO response to ENSO is found mainly during the late winter (January-February-March, JFM) (e.g., Zhang et al. 2015, 2018). Thus, we use the DJF Niño3.4 index (SSTA averaged over 5°S-5°N and 120°-170°W) as a measure of ENSO events and the JFM NAO index to characterize NAO variability. The DJF AMO is also employed (other seasonal means computed for the AMO index such as JFM or DJFM do not change the conclusion). To better isolate the inherent decadal signal of the AMO, we extract its low-frequency variability by using a 10-year low-pass fast Fourier transform (FFT) filter (other filters for the AMO index such as 9-year and 11-year low-pass filter do not change the conclusion). The linear trends of all data were removed to avoid possible influences associated with global warming. A threshold of ±0.5 standard deviations of the Niño3.4 index is used to define ENSO events. With this method we identify 20 El Niño and 24 La Niña winters (Table 1). The year in Table 1 corresponds to year(0)/year(1), which denotes the ENSO developing and decaying years, respectively. All statistical significance tests were performed based on the two-tailed Student's *t*-test.

We also analyze the Hadley Centre coupled model version 3 (HadCM3) output (1860-2005) to further verify the AMO modulation on the ENSO-NAO relationship. The model simulation, known as a "historical experiment", was driven by prescribed historical climate forcing, which includes changing atmospheric composition, solar forcing, and land use (Taylor et al. 2012). We chose the HadCM3 simulation in this study since the model has the capability to simulate both the AMO and ENSO (e.g., Lu et al. 2006; Dong et al. 2006). Since HadCM3 is a coupled model, we do not expect the phases of AMO and ENSO within it to coincide with those in observations over the 20th century; any memory of the initial state will be lost within a few years of the start of the integration.

2.2 Experimental design

In order to examine the AMO-modulation effect on the ENSO-NAO relationship, we conducted several modeling experiments based on the GFDL AM2.1 (The GFDL Global Atmospheric Model Development Team 2004) with a horizontal resolution of 2.5° longitude × 2° latitude. As a reference state, global climatological (monthly varying) SST was used to force the atmospheric model (CTRL). In addition, a group of sensitivity experiments (PAEL, NAEL, PALA and NALA) was designed (Table 2). To inspect the combined influence of the ENSO and AMO, in the PAEL experiment we added the composite SSTA for the AMO+/El Niño case on the monthly climatological SST from December to March in the tropical Pacific (30°S-30°N, 120°E-90°W) and TNA (0-30°N, 80°W-0) region (Table 2). The other three experiments (PALA, NAEL, NALA) are the same as the PAEL experiment, except that the SSTA are the composites for AMO+/La Niña, AMO-/El Niño and AMO-/La Niña cases, respectively. Each experiment was integrated for 55 years and only the last 45 years of the integrations were used to avoid any influence of the initial conditions. The differences between each sensitivity experiment and CTRL ensemble means are regarded as the specific SSTA forcing effects.

3. Observed modulation of the ENSO-NAO relationship by the AMO

Figure 1 shows the time evolution of the DJF Niño3.4 and JMF NAO indices. Conspicuous interannual variability can be found in these two indices with a weak out-of-phase relationship between them (R=-0.15, nonsignificant at the 95% confidence level). Interestingly, the negative NAO phase usually corresponds to El Niño events during the positive AMO phase. Most La Niña events accompany the positive NAO phase during a negative AMO phase. In contrast, the NAO responses to El Niño events during the negative AMO phase and La Niña events during the positive AMO phase are inconsistent. It seems that the ENSO-NAO relationship is dependent upon the AMO phase.

We next categorize ENSO events into four types according to AMO phase: that is, El Niño events during a positive AMO phase (AMO+/El Niño) and El Niño events during a negative AMO phase (AMO-/El Niño), La Niña events during a positive AMO phase (AMO+/La Niña) and La Niña events during a negative AMO phase (AMO-/La Niña) (see Table 2). Figure 2 shows the composites of anomalous winter SLP and 850 hPa horizontal winds for these four cases over the North Atlantic region. Obviously negative and positive NAO-like atmospheric circulation patterns appear over the North Atlantic for the AMO+/El Niño and AMO-/La Niña composites respectively (Figure 2a and 2d), despite a slightly westward shift of the anomalous center relative to the conventional NAO pattern. Nonetheless, no obvious NAO-like atmospheric circulation anomalies can be observed over the North Atlantic for the

AMO-/El Niño and AMO+/La Niña composites (Figure 2b and 2c). It can be seen that the NAO response is significantly strengthened (weakened) when ENSO and AMO occur as in-phase (out-of-phase) combinations. This combined effect is further examined for the AMO and ENSO based on the NCEP/NCAR 20CR reanalysis data with its longer data period. Likewise, we can also observe significant (nonsignificant) NAO-like atmospheric circulation patterns during ENSO and AMO in-phase (out-of-phase) combinations (Figure 3).

The above analyses demonstrate that the AMO plays an important role in permitting or denying the ENSO-NAO relationship. In order to clarify possible mechanisms for different NAO responses to ENSO during different AMO phases, in Figure 4 we present the regression of atmospheric circulation anomalies with respect to both AMO and ENSO indices separately, to determine if there is any similarity. The atmospheric circulation pattern regressed against the AMO index resembles the typically negative NAO-like pattern (Figure 4a), consistent with previous studies (e.g., Kavvada et al. 2013; Peings and Magnusdottir 2014). Meanwhile, the regressed SLP and wind anomalies against the Niño3.4 index also show similar negative NAO-like features over the North Atlantic. In comparison, the ENSO-related atmospheric anomalies north of 50°N are weaker and the negative NAO-like pattern cannot extend further east toward the land. The ENSO-related NAO anomalies are supported by experiments forced only by tropical Pacific SSTA of ENSO (Zhang et al. 2015, 2018). The broadly analogous atmospheric responses to ENSO and the AMO over the North Atlantic indicate a potential combined effect on NAO variability forced by ENSO and the AMO. When ENSO and the AMO occur as in-phase combinations, the NAO-like atmospheric circulation pattern should be strong and prominent. However, if ENSO and the AMO occur as out-of-phase combinations (for example, La Niña during AMO+), the NAO responses are inconsistent, resulting from offsetting effects of each other.

4. Possible modulation mechanisms associated with the AMO

We now turn to explore possible mechanisms responsible for the AMO modulation effect on the ENSO-NAO relationship. Figure 5 shows the composite anomalies of JFM SST and 1000 hPa horizontal winds for the aforementioned four cases. The SSTA during El Niño under both positive and negative AMO phases has similar patterns in the tropical Pacific, exhibiting a warming in the eastern Pacific and cooling in the surrounding regions with basically the same intensities and center positions (Figure 5a and c). Similar conditions are shown for La Niña events with positive and negative AMO phases (Figure 5b and d). Therefore, the AMO modulation effect on the ENSO pattern and intensity seems ignorable and is not considered in this study. However, Figure 5 displays very different SSTAs in the North Pacific and in the tropical and North Atlantic. Considering the high background SST, the tropical SSTA can easily excite local convection anomalies, which thus gives rise to extra-tropical atmospheric anomalies and further ocean anomalies via the "atmospheric bridge" mechanism (e.g., Alexander et al. 2002). In contrast, SSTA in the mid-latitudes is usually passive in air-sea interaction processes (Neelin et al. 1987).

So, the tropical North Atlantic may be the key region for AMO modulation of the ENSO-associated atmospheric anomalies. Here, we define the area-averaged SSTA in the tropical North Atlantic region (5°N-25°N, 15°W-55°W) as the TNA index and in Figure 6 display the spatial pattern of the regressed SLP anomaly pattern onto this TNA index. We find a distinct north-south dipole of SLP anomalies with one center located near Iceland and the other of opposite sign spanning the central latitudes of the North Atlantic between 20°N and 40°N, resembling a negative NAO-like pattern. This result is consistent with many previous studies (e.g., Brönnimann, 2007a; Peng et al. 2002, 2005). A possible mechanism suggested by Li et al. (2007) is that the TNA SSTA could excite an anomalous heating over the tropical North Atlantic, which results in a Rossby wave train propagating northeastward. Then, this wave train leads to anomalous transient-eddy activity in the North Atlantic jet exit area. This anomalous transient-eddy forcing acts linearly on the time-mean flow with a NAO-like atmospheric pattern. Thus the relatively strong TNA SSTA that occurs during AMO+/El Niño and AMO-/La Niña combinations tends to favor strong NAO responses. However, the absence of TNA SSTA during AMO-/El Niño and AMO+/La Niña combinations leads to inconsistent responses of the NAO that are not robust.

The next scientific question that remains to be answered is how this different TNA SSTA is generated. Many previous studies have shown that the TNA SST tends to increase (decrease) after the peak of El Niño (La Niña) due to an atmospheric bridge between the tropical eastern Pacific and Atlantic Oceans (e.g., Enfied and Mayer 1997; Nicholson 1997; Wang 2002). Thus, the TNA SSTA is observed to lag

ENSO by several months. The regressed North Atlantic JFM SSTA against the DJF Niño3.4 index also confirmed this well-known ENSO-teleconnected effect (figure not shown). Simultaneously, the AMO is a basin-wide dominant SSTA mode in the North Atlantic on multidecadal time scales. Therefore, when the AMO and ENSO are in phase, these two SSTA act in superposition in TNA and thus the anomaly is robust with strong signal (Figure 7). For example, under the long-term warming background SST associated with the positive AMO phase, the El Niño-associated tropical Pacific SST warming further enhances the already warm TNA SSTA (Figure 5a). This strong TNA SSTA then leads to a prominent NAO response in the atmosphere. On the contrary, when AMO and ENSO are out of phase, these two opposite-sign responses in the TNA counteract each other, resulting in a nonsignificant TNA SSTA (Figure 8) and thus an unstable NAO response.

We further examine the effect of the AMO on the ENSO-NAO relationship based on HadCM3 historical simulations (146 years) derived from the Coupled Model Intercomparison Project phase 5 (CMIP5). These simulations provide more samples of the AMO in each phase, compared to the limited observational record. The model composites of simulated JFM SLP anomalies and TNA SSTA indices for the four different phase combinations of ENSO and AMO are shown in Figures 8 and 9, respectively. During the late winter of AMO+/El Niño combinations, the positive SSTA over the TNA region is robust (Figure 9), which corresponds to significant negative NAO responses (Figure 8a). The simulated responses during AMO-/La Niña combinations in late winter are generally the opposite (Figure 8d and 9). However, neither the TNA SSTA nor the atmospheric circulation responses over the North Atlantic are obvious when the AMO and ENSO occur in out-of-phase combinations (Figure 8b-c and 9).

Finally, the combined influences of ENSO and the AMO on the NAO are confirmed by GFDL AM2.1 atmosphere-only experiments. Figure 10 shows the simulated anomalous SLP responses to the different SSTA combinations of the AMO and ENSO. It is found that obvious negative and positive NAO-like atmospheric circulation patterns appear over the North Atlantic for the PALA and NALA experiments, respectively (Figure 10a and 10d). Nevertheless, no obvious NAO-like atmospheric circulation anomalies can be simulated in the NAEL and PALA experiments (Figure 10b and 10c). These results also suggest a strong AMO modulation effect on the ENSO-NAO relationship via the TNA SSTA. The consistency between observations and model simulations increase our confidence in the aforementioned mechanism responsible for modulation of the ENSO-NAO relationship by the AMO.

5. Summary and discussion

A general physical link has been detected between ENSO and the NAO in late winter, but with a high uncertainty. In this study we demonstrate that the uncertainty of the ENSO-NAO relationship is partly due to decadal modulation by the AMO, which is therefore of importance for seasonal-to-interannual prediction of the NAO. To illustrate this AMO modulation, we categorize ENSO events into four groups according to AMO phase: AMO+/El Niño, AMO-/El Niño, AMO+/La Niña and AMO-/La Niña. It is found that when the ENSO and AMO occur as in-phase combinations (i.e., AMO+/El Niño and AMO-/La Niña), then El Niño (La Niña) events frequently correspond to significantly negative (positive) NAO-like atmospheric anomalies; this gives a significant negative ENSO-NAO relationship in late winter. In contrast, there are no significant atmospheric anomalies over the North Atlantic when ENSO and the AMO occur as out-of-phase combinations (i.e., AMO-/El Niño and AMO+/La Niña).

The tropical North Atlantic (TNA) SSTA is proposed to serve as an important medium for AMO modulation of the ENSO-NAO relationship, since it can excite remarkable NAO-like atmospheric circulation anomalies. The TNA SSTA responses to ENSO and the AMO are broadly analogous. When AMO and ENSO are in phase, their influences on the TNA SSTA occur in superposition and thus the strong TNA SSTA favors a significant NAO-associated atmospheric response. On the other hand, when AMO and ENSO are out of phase, the TNA SSTA responses counteract each other and thus the response is very weak. As a summary, a schematic (Figure 11) for the combined impacts on the NAO exerted by ENSO and the AMO is provided.

We have also checked possible effects of another prominent decadal mode in the North Pacific (i.e., the Pacific Decadal Oscillation or PDO). Almost no remarkable impacts of the PDO on the ENSO-NAO relation can be detected (not shown). In the present study, we thus emphasize the clear modulation of the ENSO-NAO relationship by the AMO. We acknowledge that many factors other than the TNA

SSTA, such as volcanic eruptions (Shindell et al. 2004; Driscoll et al. 2012), Arctic sea ice (Hilmel and Jung 2000; Seierstad and Bader 2009) and internal atmospheric variability (Kumar and Hoerling 1998), may also impact the NAO-related atmospheric circulation. In addition, ENSO itself exhibits a considerable degree of diversity in its SSTA pattern, which also complicates its connection with the NAO (e.g., Greatbatch et al. 2004; Graf and Zanchettin 2012; Zhang et al. 2015, 2018). All these factors may increase the uncertainty of the ENSO-NAO relationship.

Acknowledgements

This work was supported by the National Nature Science Foundation of China (41675073), the SOA Program on Global Change and Air-Sea interactions (GASI-IPOVAI-03). AGT was supported by the NCAS-Climate Core Agreement, Contract number R8/H12/83/00.

REFERENCES

Alexander, L. V., X. Zhang, T. C. Peterson, J. Caesar, and B. Gleason, 2006: Global observed changes in daily climate extremes of temperature and precipitation. *J. Geophys. Res.*, **111**, D05109.

Alexander, M. A., I. Blade, M. Newman, J. R. Lanzante, N.-C. Lau and J. D. Scott 2002: The atmospheric bridge: The influence of ENSO teleconnections on air-sea interaction over the global oceans, *J. Clim.*, **15**, 2205-2231.

Bell, C. J., L. J. Gray, A. J. Charlton-Perez, M. M. Joshi, and A. A. Scaife, 2009: Stratospheric communication of El Niño teleconnections to European winter. *J. Clim.*, **22**, 4083-4096.

Brönnimann, S., 2007a: Impact of El Niño-Southern Oscillation on European, *climate. Rev. Geophys.*, **45**, RG3003.

——, E. Xoplaki, C. Casty, A. Pauling, and J. Luterbacher, 2007b: ENSO influence on Europe during the last centuries. *Clim. Dyn.*, **28**, 181-197.

Castanheira, J. M., and H. F. Graf, 2003: North Pacific-North Atlantic relationships under stratospheric control? *J. Geophys. Res.*, **108**, 4036, doi:10.1029/2002JD002754.

Cattiaux, J., R. Vautard, C. Cassou, P. Yiou, V. Masson-Delmotte, and F. Codron, 2010: Winter 2010 in Europe: A cold extreme in a warming climate. *Geophys. Res. Lett.,* **37**, L20704.

Cohen, J. L., J. C. Furtado, M. A. Barlow, V. A. Alexeev, and J. E. Cherry, 2012: Arctic warming, increasing snow cover and widespread boreal winter cooling. *Environ. Res. Lett.*, **7**, 011004.

Compo, G. P., J. S. Whitaker, P. D. Sardeshmukh, N. Matsui, and R. J. Allan, 2011: . *Quarterly J. Roy. Meteorol. Soc.*, **137**, 1-28.

Davini, P., J. Hardenberg, and S. Corti, 2015: Tropical origin for the impacts of the Atlantic Multidecadal Variability on the Euro-Atlantic climate. *Environ. Res. Lett.*, **10**, 094010.

Deser, C., and H. Teng, 2008: Evolution of Arctic sea ice concentration trends and the role of atmospheric circulation forcing, 1979-2007. *Geophys. Res. Lett.*, **35**, L02504.

Dong, B. W., R. T. Sutton and A. A. Scaife, 2006: Multidecadal modulation of El Niño-Southern Oscillation (ENSO) variance by Atlantic Ocean sea surface temperatures. *Geophys. Res. Lett.*, **33**, L08705.

Driscoll, S., A. Bozzo, L. G. Gray, A. Robock, and G. Stenchikov 2012: Coupled Model Intercomparison Project 5 (CMIP5) simulations of climate following volcanic eruptions. *J. Geophys. Res.*, **117**, 127-135.

Drouard. M., G. Riviere, and P. Arbogast, 2015: The link between the North Pacific climate variability and the North Atlantic Oscillation via downstream propagation of synoptic waves. *J. Clim.*, **28**, 3957-3976.

Dunstone, N., D. Smith, A. Scaife, L. Hermanson, R. Eade, N. Robinson, M. Andrews, and J. Knight, 2016: Skilful predictions of the winter North Atlantic Oscillation one year ahead. *Nat. Geosci.*, **9**, 809-814.

Enfield, D. B., A. M. Mestas-Nuñez, and P. J. Trimble, 2001: The Atlantic multidecadal oscillation and its relation to rainfall and river flows in the continental US. *Geophys. Res. Lett.*, **28**, 2077-2080.

——, and D. A. Mayer, 1997: Tropical Atlantic sea surface temperature variability and its relation to El Niño-Southern Oscillation. *J. Geophys. Res.*, **102**, 929-945.

Fraedrich, K., and K. Muller, 1992: Climate anomalies in Europe associated with ENSO extremes. *Int. J. Climatol.*, **12**, 25-31.

——, 1994: An ENSO impact on Europe? Tellus, **46A**, 541-552.

Geng, X., W. J. Zhang., M. F. Stuecker, and F. F. Jin, 2017: Strong sub-seasonal wintertime cooling over East Asia and Northern Europe associated with super El Niño events. *Sci. Rep.*, **7**, doi: 10.1038/s41598-017-03977-2.

Gouirand, I., and V. Moron, 2003: Variability of the impact of El Niño-Southern Oscillation on sea-level pressure anomalies over the North Atlantic in January to March (1874-1996). *Int. J. Climatol.*, **23**, 1549-1566.

Graf, H. F., and D. Zanchettin, 2012: Central Pacific El Niño, the"subtropical bridge", and Eurasian climate. *J. Geophys. Res.*, **117**, D01102.

Greatbatch, R. J., J. Lu, and K. A. Peterson, 2004: Nonstationary impact of ENSO on Euro-Atlantic winter climate. *Geophys. Res. Lett.*, **31**, L02208.

Groisman, P. Y., and E. Y. Rankova, 2001: Precipitation trends over the Russian permafrost-free zone: Removing the artifacts of pre-processing. *Int. J. Climatol.*, **21**, 657-678.

——, R. W. Knight, D. R. Easterling, T. R. Karl, G. C. Hegerl, and V. N. Razuvaev 2005: Trends in intense precipitation in the climate record. *J. Clim.*, **18**, 1326-1350.

Hilmel, M., and T. Jung, 2000: Evidence for a recent change in the link between the North Atlantic Oscillation and Arctic sea ice export. *Geosphy. Res. Lett.*, **27**, 989-992.

Hurrell, J. W., 1995: Decadal trends in the North-Atlantic oscillationregional temperatures and precipitation. Science, **269**, 676-679.

——, 1996: Influence of variations in extratropical wintertime teleconnections on Northern Hemisphere temperature. *Geophys. Res. Lett.*, **23**, 665-668.

——, Y. Kushnir, G. Ottersen, and M. Visbeck, 2003: An overview of the North Atlantic Oscillation. In: Hurrell, J. W., Y. Kushnir, G. Ottersen, and M. Visbeck, (eds) The North Atlantic Oscillation: climate significance and environmental impact. American Geophysical Union, Washington, pp 1-35.

Ineson, S., and A. A. Scaife, 2009: The role of the stratosphere in the European climate response to El Niño. *Nat. Geosci.*, **2**, 32-36.

Infanti, J. M., and B. P. Kirtman, 2016: North American rainfall and temperature prediction response to the diversity of ENSO. *Clim. Dyn.*, **46**, 3007-3023.

Johansson, A., 2007: Prediction Skill of the NAO and PNA from Daily to Seasonal Time Scales. *J. Clim*., **20**, 1957-1975.

Kalnay, E., M. Kanamitsu, R. Kistler, and W. Collins, 1996: The NCEP/NCAR 40-year reanalysis project. *Bull. Am. Meteorol. Soc.*, **77**, 437-471.

Kavvada, A., A. Ruiz-Barradas, and S. Nigam, 2013: AMO's structure and climate footprint in observations and IPCC AR5 climate simulations. *Clim. Dyn.*, **41**, 1345-1364.

Kerr, R. A., 2000: A North Atlantic climate pacemaker for the centuries. Science, **288**, 1984-1986.

Klein, S. A., B. J. Soden, and N. -C. Lau, 1999: Remote sea surface temperature variations during ENSO: Evidence for a tropical atmospheric bridge. *J. Clim.*, **12**, 917-932.

Kumar, A., and M. P. Hoerling, 1998: Annual cycle of Pacific/North American seasonal predictability associated with different phases of ENSO. *J. Clim.*, **11**, 3295-3308.

Lau, N. -C., and M. J. Nath, 2003: Atmosphere-ocean variations in the Indo-Pacific sector during ENSO episodes. *J. Clim.*, **16**, 3-20.

Li, J. P., and J. X. L. Wang, 2003: A new North Atlantic Oscillation index and its variability. *Adv. Atmos. Sci.*, **20**, 661-676.

——, C. Sun, and F. F. Jin, 2013: NAO implicated as a predictor of Northern Hemisphere mean temperature multidecadal variability. *Geophys. Res. Lett.*, **40**, 5497-5502.

——, and C. Q. Ruan, 2018: The North Atlantic-Eurasian teleconnection in summer and its effects on Eurasian climates. *Environ. Res. Lett.*, **13**, 024007.

Li., S. L., W. A. Robinson, M. P. Hoerling, and K. M. Weickmann, 2007: Dynamics of the extratropical response to a tropical Atlantic SST anomaly. *J. Clim.*, **20**, 560-574.

Li, Y., and N. -C. Lau, 2012a: Impact of ENSO in the atmospheric variability over the North Atlantic in late winter-role of transient eddies. *J. Clim.*, **25**, 320-342.

——, and N. -C. Lau, 2012b: Contributions of downstream eddy development to the teleconnection between ENSO and the atmospheric circulation over the North Atlantic. *J. Clim.*, **25**, 4993-5010.

Lu, R. Y., B. W. Dong and H. Ding, 2006: Impact of the Atlantic Multidecadal Oscillation on the Asian summer monsoon. *Geophys. Res. Lett.*, **33**, L24701.

Mathieu, P. P., R. T. Sutton, B. W. Dong, and M. Collins, 2004: Predictability of winter climate over the North Atlantic European region during ENSO events. *J. Clim.*, **17**, 1953-1974.

Moron, M. and G. Plaut, 2003: The impact of El Niño Southern Oscillation upon weather regimes over Europe and the North Atlantic boreal winter. *Int. J. Climatol.*, **23**, 363-379.

Moron, V. and I. Gouirand, 2003: Seasonal modulation of the El Niño Southern Oscillation relationship with sea level pressure anomalies over the North Atlantic in October-March 1873-1996. *Int. J. Climatol.*, **23**, 143-155.

Msadek, R., C. Frankignoul, and L. Li, 2011: Mechanisms of the atmospheric response to North Atlantic multidecadal variability: a model study. *Clim. Dyn.*, **36**, 1255-1276.

Neelin, J. D., I. M. Held and K. H. Cook, 1987: Evaporation-wind feedback and low-frequency variability in the tropical atmosphere. *J. Atmos. Sci.*, **44**, 2341-2348.

Nicholson, S. E., 1997: An analysis of the ENSO signal in the Tropical Atlantic and Western Indian Ocean. *Int. J. Climatol.*, **17**, 345-375.

Omrani, N. E., N. S. Keenlyside, J. Bader, and E. Manzini, 2014: Stratosphere key for wintertime atmospheric response to warm Atlantic decadal conditions. *Clim. Dyn.*, **42**, 649-663.

Peings, Y., and G. Magnusdottir, 2014: Forcing of the wintertime atmospheric circulation by the multidecadal fluctuations of the North Atlantic Ocean. *Environ. Res. Lett.*, **9**, 034018.

Peng, S. L., W. A. Robinson, and S. L. Li, 2002: North Atlantic SST forcing of the NAO and relationships with intrinsic hemispheric variability. *Geophys. Res. Lett.*, **29**, doi:10.1029/2001GL014043.

——, ——, ——, and M. P. Hoerling, 2005 Tropical Atlantic SST Forcing of Coupled North Atlantic Seasonal Responses. *J. Clim.*, **18**, 480-496.

Robertson, A. W., and C. R. Mechoso, and Y. J. Kim, 2000: The influence of the Atlantic sea surface temperature anomalies on the North Atlantic Oscillation. *J. Clim.*, **13**, 122-138.

Ropelewski, C. F., and M. S. Halpert, 1987: Global and regional scale precipitation patterns associated with the El Niño/Southern Oscillation. *Mon. Weather Rev.*,

115, 1606-1626.

Scaife, A. A., C. K. Folland, L. V. Alexander, A. Moberg, and J. R. Knight, 2008: European climate extremes and the North Atlantic Oscillation. *J. Clim.*, **21** 72-83.

Seierstad, I. A., and J. Bader, 2009: Impact of a projected future Arctic Sea Ice reduction on extratropical storminess and the NAO. *Clim. Dyn.*, **33**, 937-943.

Shindell, D. T., G. A. Schmidt, M. E. Mann, and G. Faluvegi 2004: Dynamic winter climate response to large tropical volcanic eruptions since 1600. *J. Geophys. Res.*, **109**, D05104.

Smith, D. M., A. A., Scaife, R. Eade, and J. R. Knight, 2016: Seasonal to decadal prediction of the winter North Atlantic Oscillation: emerging capability and future prospects. *Q. J. R. Meteorol. Soc.*, **142**, 611-617.

Smith, T. M., R. W. Reynolds, T. C. Peterson, and J. Lawrimore, 2008: Improvements to NOAA’s historical merged land-ocean surface temperature analysis (1880-2006). *J. Clim.*, **21**, 2283-2296.

Stenchikov, G., K. Hamilton, R. J. Stouffer, A. Robock, V. Ramaswamy, B. Santer, and H. F. Graf, 2006: Arctic Oscillation response to volcanic eruptions in the IPCC AR4 climate models. *J. Geophys. Res.*, **111**, D07107.

Sun, Y. B., S. C. Clemens, C. Morrill, X. Lin, X. Wang, and Z. An, 2011: Influence of Atlantic meridional overturning circulation on the East Asian winter monsoon. *Nat. Geosci.*, **5**, 46-49.

Sun, C., J. P. Li, and F. F. Jin, 2015: A delayed oscillator model for the quasiperiodic multidecadal variability of the NAO. *Clim. Dyn.*, **45**, 2083-2099.

Sutton, R. T., B. Dong, 2012: Atlantic Ocean influence on a shift in European climate in the 1990s. *Nat. Geosci.*, **5**, 788-792.

——, and D. L. R. Hodson, 2005: Atlantic Ocean forcing of North American and European summer climate. *Science*, **309**, 115-118.

Taylor, K. E., R. J. Stouffer, and G. A. Meehl, 2012: An Overview of CMIP5 and the Experiment Design. *Bull. Amer. Meteor. Soc.*, **93**, 485-498.

The GFDL Global Atmospheric Model Development Team, 2004: The New GFDL

Global Atmosphere and Land Model AM2-LM2: evaluation with prescribed SST simulations. *J. Clim.*, **17**, 4641-4673.

Thompson, D. W. J., and J. M. Wallace, 2000: Annular modes in the extratropical circulation. Part I: month-to-month variability. *J. Clim.*, **13**, 1000-1016.

Ting, M. F., Y. Kushnir, R. Seager, and C. H. Li, 2011: Robust features of Atlantic multi-decadal variability and its climate impacts. *Geophys. Res. Lett.*, **38**, L17705.

——, Y. Kushnir, and C. H. Li, 2014: North Atlantic Multidecadal SST Oscillation: External forcing versus internal variabilit. *J. Mar. Sys.*, **133**, 27-38.

Toniazzo, T., and A. A. Scaife, 2006: The influence of ENSO on winter North Atlantic climate. *Geophys. Res. Lett.*, **33**, L24704.

Wang, C. Z., 2002: Atlantic climate variability and its associated atmospheric circulation cells. *J. Clim.*, **15**, 1516-1536.

——, and J. Picaut, 2004: Understanding ENSO physics-A review, in Earth's Climate: The Ocean-Atmosphere Interaction. *Geophys. Monogr. Ser.*, **147**, 21-48.

——, H. Liu, and S. -K. Lee, 2010: The record-breaking cold temperatures during the winter of 2009/2010 in the Northern Hemisphere. *Atmos. Sci. Lett.*, **11**, 161-168.

Watanabe, M., and M. Kimoto, 1999: Tropical-extratropical connection in the Atlantic atmosphere-ocean variability. *Geophys. Res. Lett.*, **26**, 2247-2250.

Wettstein, J. J., and L. O. Mearns, 2002: The influence of the North Atlantic-Arctic Oscillation on mean, variance, and extremes of temperature in the northeastern United States and Canada. *J. Clim.*, **15**, 3586-3600.

Wu. A., and W. W. Hsieh, 2004: The nonlinear association between ENSO and the Euro-Atlantic winter sea level pressure. *Clim. Dyn.*, **23**, 859-868.

Zhang, R., T. L. Delworth, and I. M. Held, 2007: Can the Atlantic Ocean drive the observed multidecadal variability in Northern Hemisphere mean temperature? *Geophys. Res. Lett.*, **34**, L02709.

Zhang, W. J., L. Wang, B. Q. Xiang, L. Qi and J. H. He, 2015a: Impacts of two types of La Niña on the NAO during boreal winter. *Clim. Dyn.*, **44**, 1351-1366.

——, Z. Q. Wang, M. F. Stuecker, A. G. Turner, F. F. Jin, and X. Geng, 2018: Impact of ENSO longitudinal position on teleconnections to the NAO. *Clim. Dyn.*, http://doi.org/10.1007/s00382-018- 4135-1.

Table 1. El Niño and La Niña events for the 1950-2016 period based on the Niño3.4 index.

El Niño events	La Niña events
1953/54, 1957/58, 1963/64, 1965/66, 1968/69, 1969/70, 1972/73, 1976/77, 1977/78, 1982/83, 1986/87, 1987/88, 1991/92, 1994/95, 1997/98, 2002/03, 2004/05, 2006/07, 2009/10, 2015/16	1950/51, 1954/55, 1955/56, 1962/63, 1964/65, 1967/68, 1970/71, 1971/72, 1973/74, 1974/75, 1975/76, 1984/85, 1988/89, 1995/96, 1998/999, 1999/00, 2000/01, 2005/06, 2007/08, 2008/09, 2010/11, 2011/2012, 2012/2013, 2013/2014

Table 2. List of the conducted SST perturbation experiment

Experiment	Description of the SST perturbation
PAEL	Composite SST anomalies for the AMO+/El Niño case are imposed on the monthly climatological SST from December to March in the tropical Pacific (30°S-30°N, 120°E-90°W) and the tropical North Atlantic (0-30°N, 80°W-0) regions.
NAEL	As in PAEL but the composite SST anomalies for the AMO-/El Niño case are imposed.
PALA	As in PAEL but the composite SST anomalies for the AMO+/La Niña case are imposed.
NALA	As in PAEL but the composite SST anomalies for the AMO-/La Niña case are imposed.

Table 3. Category of El Niño and La Niña events for the 1950-2016 period according to AMO phase.

Categories	Years
AMO+/El Niño	1953/54, 1957/58, 1963/64, 1965/66, 1997/98, 2002/03, 2004/05, 2006/07, 2009/10, 2015/16
AMO-/El Niño	1968/69, 1969/70, 1972/73, 1976/77, 1977/78, 1982/83, 1986/87, 1987/88, 1991/92, 1994/95
AMO+/La Niña	1950/51, 1954/55, 1955/56, 1962/63, 1964/65, 1998/999, 1999/00, 2000/01, 2005/06, 2007/08, 2008/09, 2010/11, 2011/2012, 2012/2013, 2013/2014
AMO-/La Niña	1967/68, 1970/71, 1971/72, 1973/74, 1974/75, 1975/76, 1984/85, 1988/89, 1995/96

Figure Captions

Figure 1. Time evolution of JFM NAO (blue solid line), DJF Niño3.4 (red dashed line) and DJF AMO (bar) indices from 1950/51 to 2015/16 winter. Orange and green dots represent the El Niño and La Niña winters, respectively. The decadal component of AMO index is shown here, which is calculated using a 10-year low-pass filter.

Figure 2. Composites of anomalous SLP (contours in hPa, from -4.0 to 3.0 by 1.0) and 850 hPa horizontal winds (vector in m/s) for (a) AMO+/El Niño; (b) AMO+/La Niña; (c) AMO-/El Niño; (d) AMO-/La Niña cases based on NCEP/NCAR reanalysis data. Shading represents those SLP anomalies above the 90%, 95% and 99% confidence levels, respectively. The wind anomalies are only displayed when the zonal or meridional wind anomalies are significant at the 90% confidence level.

Figure 3. As in Figure 2, but for composites based on 20CR data in the period of 1900-2012 (contour in hPa, from -3.0 to 3.0 by 1.0).

Figure 4. Regressed anomalous patterns of SLP (contour in hPa, from -0.8 to 1.6 by 0.4) and 850 hPa horizontal winds (vector in m/s) with respect to the (a) AMO and (b) Niño3.4 indices. Shading represents those SLP anomalies significant above the 90%, 95% and 99% confidence levels, respectively. The wind anomalies are shown only when the zonal or meridional wind anomalies are significant at the 90% confidence level.

Figure 5. Composites of anomalous SST (shading in °C) and 1000 hPa horizontal

wind (vector in m/s) for the (a) AMO+/El Niño, (b) AMO+/La Niña, (c) AMO-/El Niño, (d) AMO-/La Niña cases. Shading represents those SST anomalies significant above the 90%, 95% and 99% confidence levels, respectively. The wind anomalies are only displayed when the zonal or meridional wind anomalies are significant at the 90% confidence level. The yellow box (15°W-55°W, 5°N-25°N) is the domain used to define the tropical North Atlantic (TNA) index.

Figure 6. Regressed anomalous patterns of JFM SLP (contour in hPa, from -1.6 to 3.2 by 0.8) with respect to the simultaneous TNA index. Shading represents those SLP anomalies significant above the 90%, 95% and 99% confidence levels, respectively. The yellow box is the domain used to define the tropical North Atlantic (TNA) index.

Figure 7. Composites of tropical North Atlantic (TNA) indices for AMO+/El Niño, AMO+/La Niña, AMO-/El Niño, and AMO-/La Niña cases. The error bars represent one standard deviation error estimates.

Figure 8. As in Figure 2, but for composites based on the HadCM3 historical simulations (contour in hPa, from -3.0 to 1.0 by 0.5).

Figure 9. As in Figure 7, but for composites based on the HadCM3 historical simulations.

Figure 10. AM2.1 simulated JFM anomalous SLP (contour in hPa, from -4.0 to 5.0 by 1.0) responses to (a) PAEL, (b) PALA, (c) NAEL and (d) NALA SSTA forcings. Shading represents those SLP anomalies significant above the 90%, 95% and 99%

confidence levels, respectively.

Figure 11. Schematic for AMO modulation of the ENSO-NAO relationship. "+" and "-" indicates the positive and negative phase, respectively. For instance, ENSO+ and ENSO- represent the positive ENSO phase (i.e., El Niño) and the negative ENSO phase (i.e., La Niña).

List of Figures

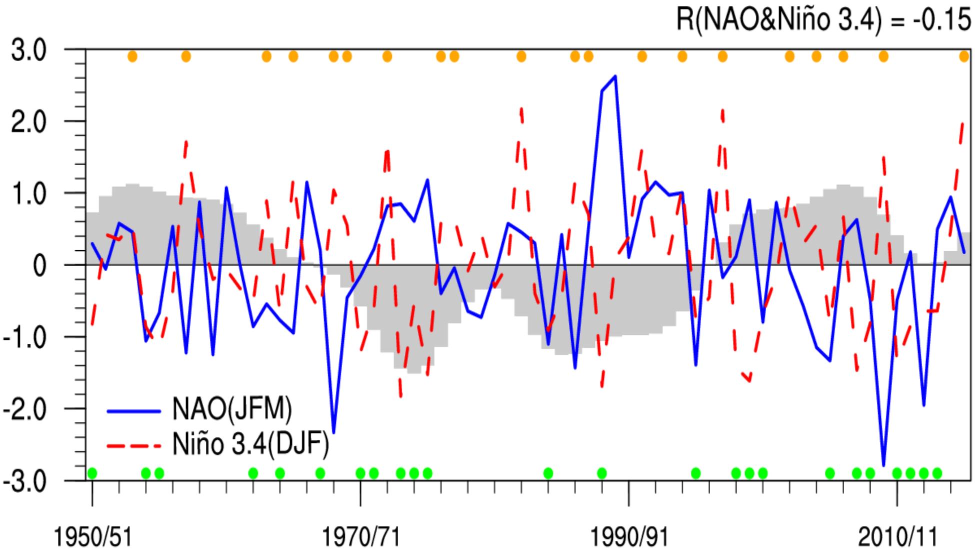

Figure 1. Time evolution of JFM NAO (blue solid line), DJF Niño3.4 (red dashed line) and DJF AMO (bar) indices from 1950/51 to 2015/16 winter. Orange and green dots represent the El Niño and La Niña winters, respectively. The decadal component of AMO index is shown here, which is calculated using a 10-year low-pass filter.

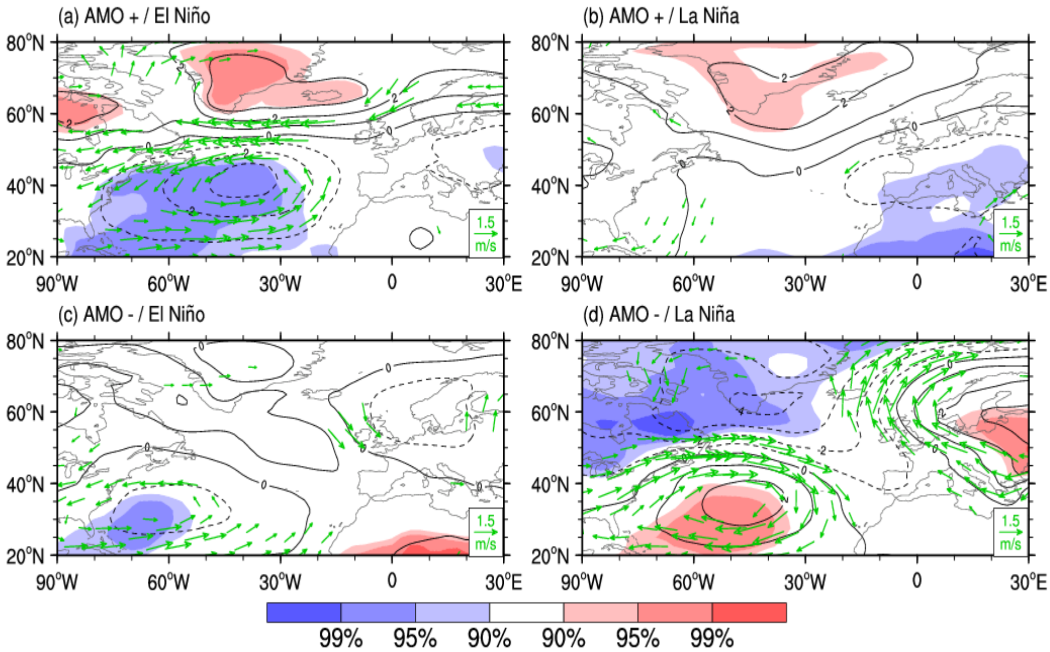

Figure 2. Composites of anomalous SLP (contours in hPa, from -4.0 to 3.0 by 1.0) and 850 hPa horizontal winds (vector in m/s) for (a) AMO+/El Niño; (b) AMO+/La Niña; (c) AMO-/El Niño; (d) AMO-/La Niña cases based on NCEP/NCAR reanalysis data. Shading represents those SLP anomalies significant above the 90%, 95% and 99% confidence levels, respectively. The wind anomalies are only displayed when the zonal or meridional wind anomalies are significant at the 90% confidence level.

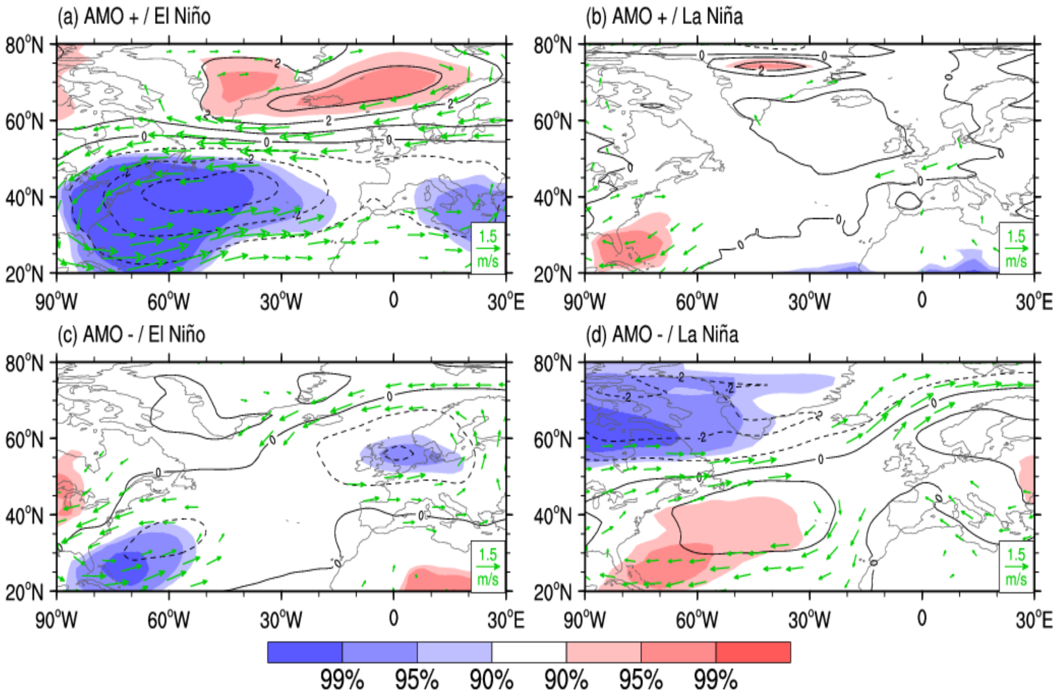

Figure 3. As in Figure 2, but for composites based on 20CR data in the period of 1900-2012 (contour in hPa, from -3.0 to 3.0 by 1.0).

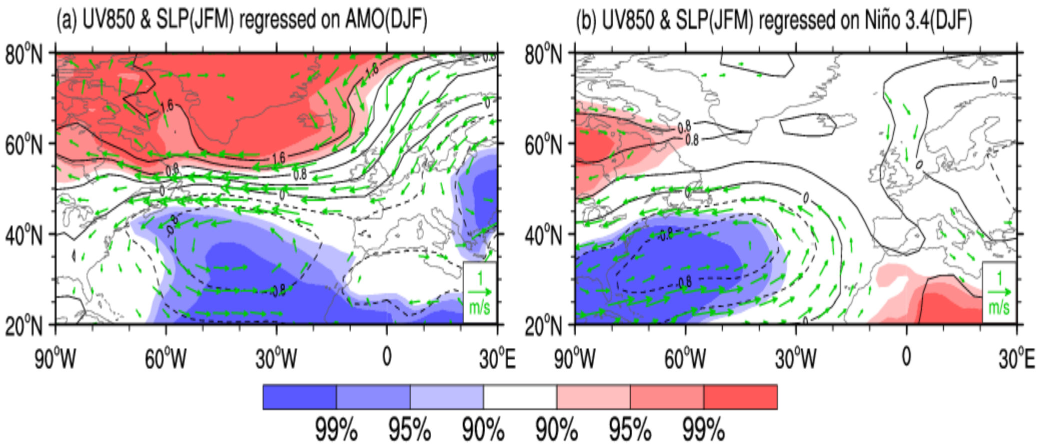

Figure 4. Regressed anomalous patterns of SLP (contour in hPa, from -0.8 to 1.6 by 0.4) and 850 hPa horizontal winds (vector in m/s) with respect to the (a) AMO and (b) Niño3.4 indices. Shading represents those SLP anomalies significant above the 90%, 95% and 99% confidence levels, respectively. The wind anomalies are shown only when the zonal or meridional wind anomalies are significant at the 90% confidence level.

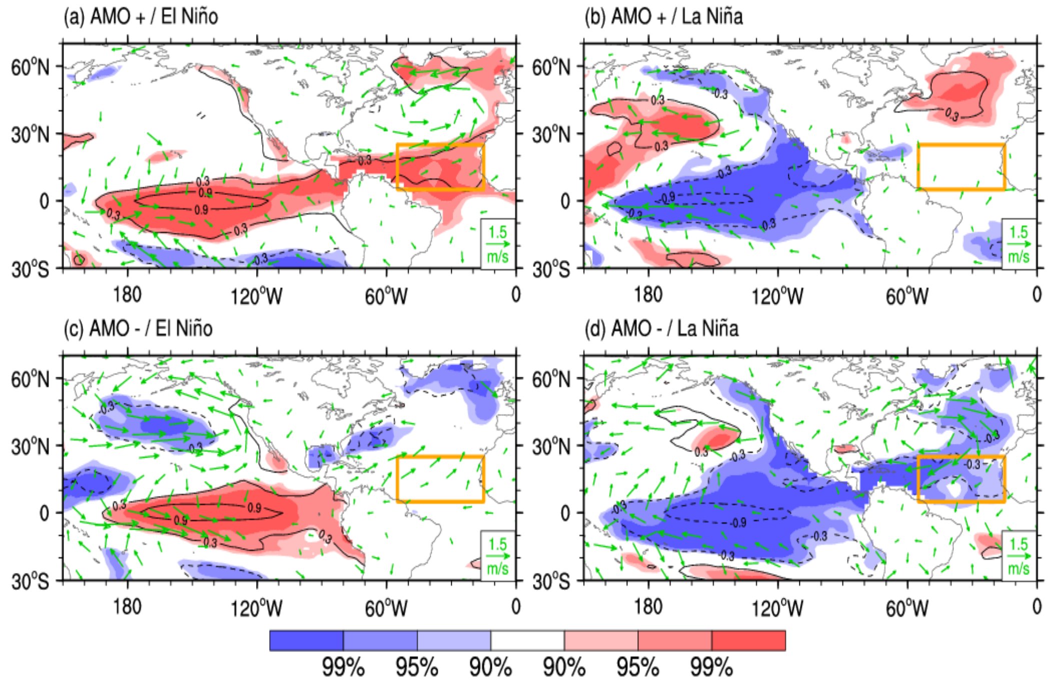

Figure 5. Composites of anomalous SST (shading in °C) and 1000 hPa horizontal wind (vector in m/s) for the (a) AMO+/El Niño, (b) AMO+/La Niña, (c) AMO-/El Niño, (d) AMO-/La Niña cases. Shading represents those SST anomalies significant above the 90%, 95% and 99% confidence levels, respectively. The wind anomalies are only displayed when the zonal or meridional wind anomalies are significant at the 90% confidence level. The yellow box (15°W-55°W, 5°N-25°N) is the domain used to define the tropical North Atlantic (TNA) index.

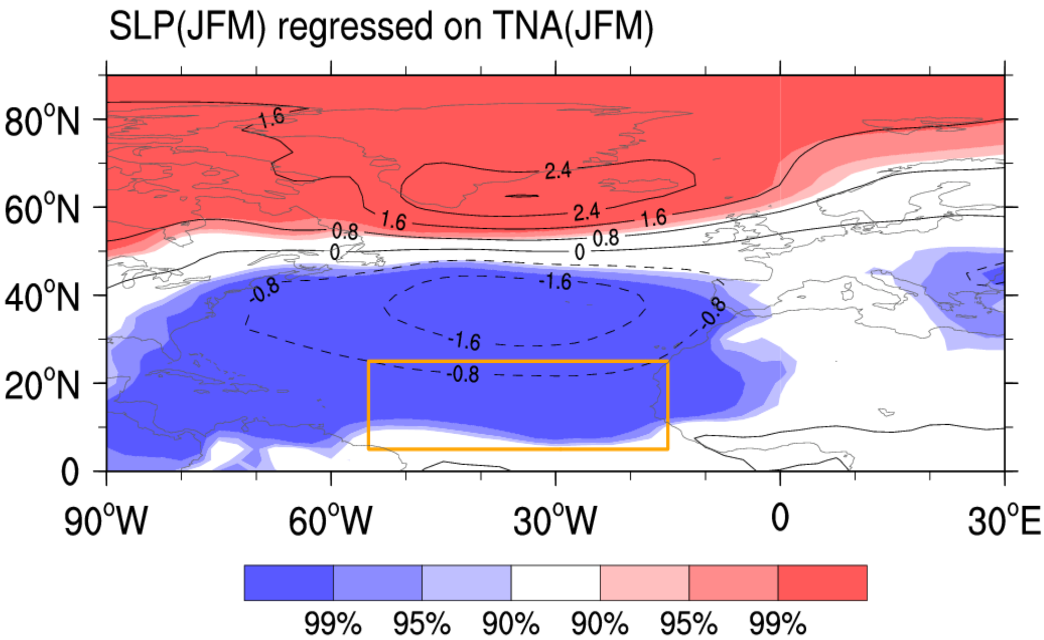

Figure 6. Regressed anomalous patterns of JFM SLP (contour in hPa, from -1.6 to 3.2 by 0.8) with respect to the simultaneous TNA index. Shading represents those SLP anomalies significant above the 90%, 95% and 99% confidence levels, respectively. The yellow box is the domain used to define the tropical North Atlantic (TNA) index.

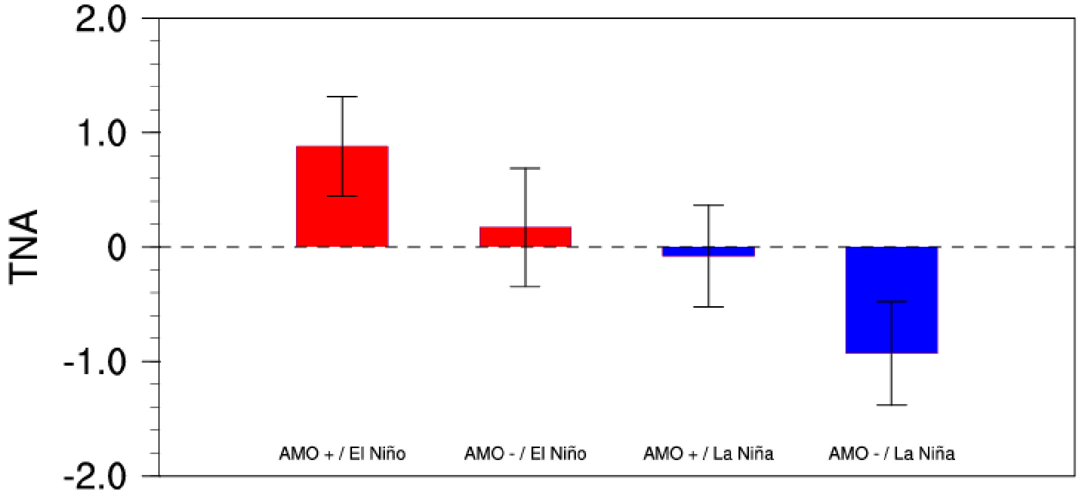

Figure 7. Composites of tropical North Atlantic (TNA) indices for the AMO+/El Niño, AMO+/La Niña, AMO-/El Niño, AMO-/La Niña cases. The error bars represent one standard deviation error estimates.

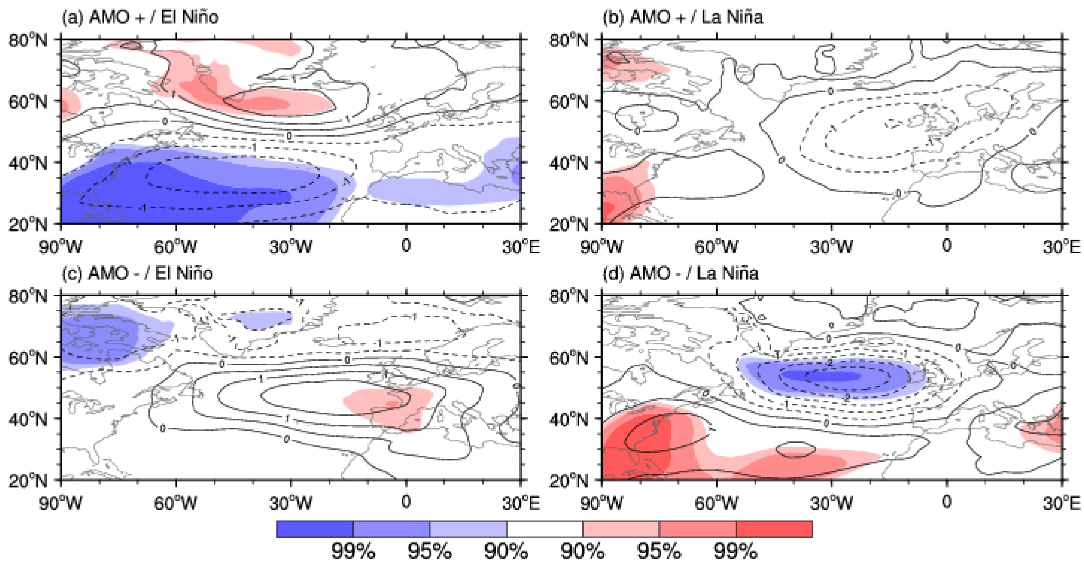

Figure 8. As in Figure 2, but for composites based on the HadCM3 historical simulations (contour in hPa, from -3.0 to 1.0 by 0.5).

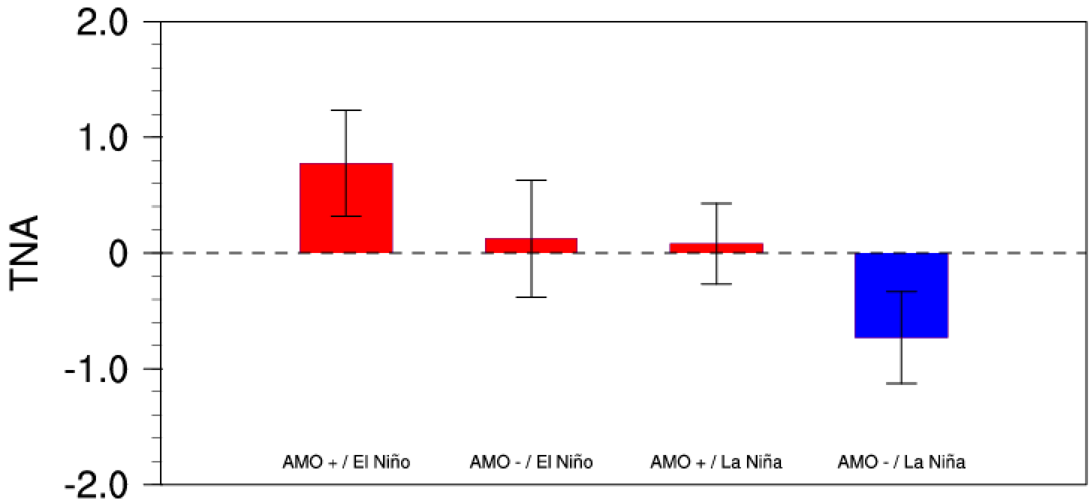

Figure 9. As in Figure 7, but for composites based on the HadCM3 historical simulations.

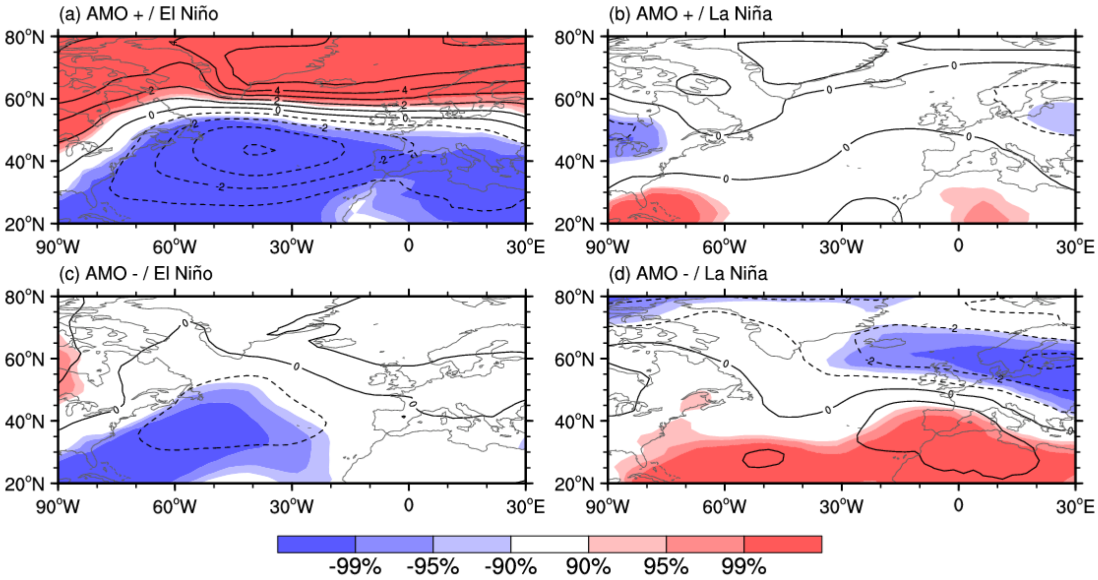

Figure 10. AM2.1 simulated JFM SLP responses (contour in hPa, from -4.0 to 5.0 by 1.0) to (a) PAEL, (b) PALA, (c) NAEL and (d) NALA SSTA forcings. Shading represents those SLP anomalies significant above the 90%, 95% and 99% confidence levels, respectively.

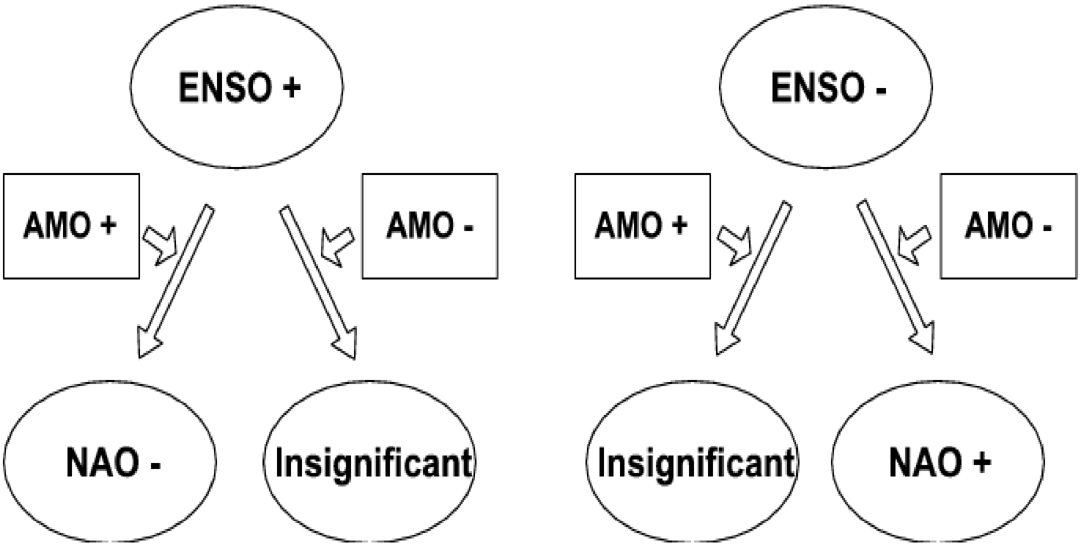

Figure 11. Schematic for AMO modulation of the ENSO-NAO relationship. “+” and “-“ indicates the positive and negative phase, respectively. For instance, ENSO+ and ENSO- represent the positive ENSO phase (i.e., El Niño) and the negative ENSO phase (i.e., La Niña).